Radiative Structures of Lycopodium-Air Flames in Low Gravity

A. L. Berlad* and V. Tangirala†
University of California, San Diego, La Jolla, California 92093
and
H. Ross‡ and L. Facca‡
NASA Lewis Research Center, Cleveland, Ohio 44135

Initially uniform clouds of fuel particulates in air sustain processes which may lead to particle-cloud nonuniformities. In low gravity, flame-induced Kundt's tube phenomena are observed to form regular patterns of nonuniform particle concentrations. Irregular patterns of particle concentrations also are observed to result from selected nonuniform mixing processes. Low-gravity flame propagation for each of these classes of particle-cloud flames has been found to depend importantly on the flame-generated infrared radiative fields. The spatial structures of these radiative fields are described. Application is made for the observed cases of lycopodium-air flames.

Introduction

THE combustion of clouds of fuel particulates in an oxidizing gaseous atmosphere is of broad scientific and practical interest. For gaseous systems, combustion characteristics such as flame structure, quasisteady flame-propagation rates, ignition energy, flammability limits, etc., are routinely observed for easily established premixed quiescent systems. Contrastingly, for a combustible system containing clouds of particulates, sedimentation processes intrinsic to normal Earth-gravity (g_0) conditions make it difficult or impossible to establish corresponding premixed quiescent systems. However, reduced-gravity conditions ($g \leq 0.01\, g_0$) permit establishment of adequately uniform and quiescent clouds of fuel particulates.[1-4] The NASA Lewis Research Center drop tower, as well as Learjet research aircraft, has been employed to create clouds of fuel particulates suitable for the study of low-gravity flame-propagation phenomena. Flame propagation sustained by quiescent clouds of lycopodium particles in air have been observed. This report is intended to delineate the essential roles played by the flame's radiative field (and by the optical attenuation properties of the fuel particulates) in the flame-propagation modes observed.

Experimental Arrangement on the Learjet

The experimental arrangement is essentially that described in Ref. 2. A long flame tube is Learjet mounted and contains a premeasured lycopodium particulate charge. The initially sealed flame tube contains air at atmospheric pressure. As noted previously,[2] the experiment is run in four stages, during approximately 20 s of low g available on a Learjet in a Keplerian trajectory: 1) an acoustic driver is turned on to mix the particles into a suitably uniform cloud; 2) the driver is turned off, and secondary airflows given time to decay; 3) a nitrocellulose igniter is powered, burning through a mylar diaphragm and igniting the particle cloud; and 4) flame propagation proceeds axially down the tube length.

Four LED optical detectors measure cloud uniformity. High-speed (200 frames/s) photography provides details of flame propagation. Figure 1 is a schematic of the flame-tube apparatus.

Experimental Results

An initially uniform and quiescent unburned particle cloud is desired[1,5] to support quasisteady flame propagation. Figure 2 shows the optical attenuation record of a well-mixed particle cloud, as measured by four LED detectors, distributed along the length of the flame tube. For the case shown, time is measured after the cessation of the 0.5-s acoustic burst which is used to initiate the mixing process. After about a 10-s period provided for the decay of the mixing-related secondary flows, flame propagation is initiated. The fine ash-containing reaction zone regime provides only weak attenuation of the optical detector signals. Cold, unburned, particle-laden gas is a strong attenuator. Accordingly, rapid decreases in optical attenuation signals occur in rapid sequence: first at detector number 1 (closest to the nichrome igniter) and finally at detector number 4 (near the closed end of the tube). Figure 2 corresponds to an overall equivalence ratio, $\phi_0 = 1.21$, and is illustrative of an acceptable particle uniformity (prior to combustion), which subsequently supports an acoustically excited flame within which particle segregation occurs.

During the course of Learjet-based experimentation, several interesting flame-propagation modes have been observed. Each mode is strongly dependent on the radiative fields peculiar to its unique flame structure. Each of the three flame-propagation modes illustrated in Fig. 3 corresponds to a particle-cloud system for which (large spatial scale) particle mass density is effectively uniform.

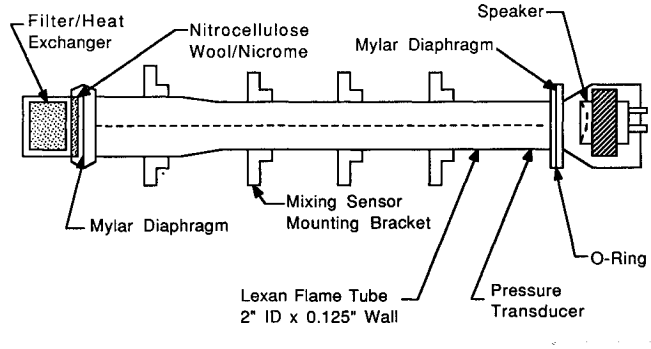

Fig. 1 Schematic of the flame-tube assembly. Flame propagates from left to right.

Presented as Paper 89-0500 at the AIAA 27th Aerospace Sciences Meeting, Reno, NV, Jan. 9-12, 1989; received March 13, 1989; revision received Sept. 29, 1989.

*Professor, Center for Energy and Combustion Research. Member AIAA.
†Research Engineer, Center for Energy and Combustion Research.
‡Research Scientist.

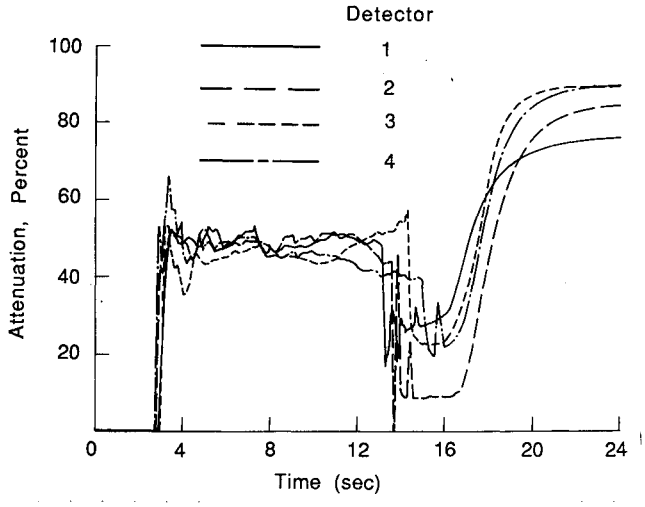

Fig. 2 Learjet experiment 13. Particle-cloud optical attenuation during cloud mixing and combustion at reduced gravity. (Flame propagates from left to right.)

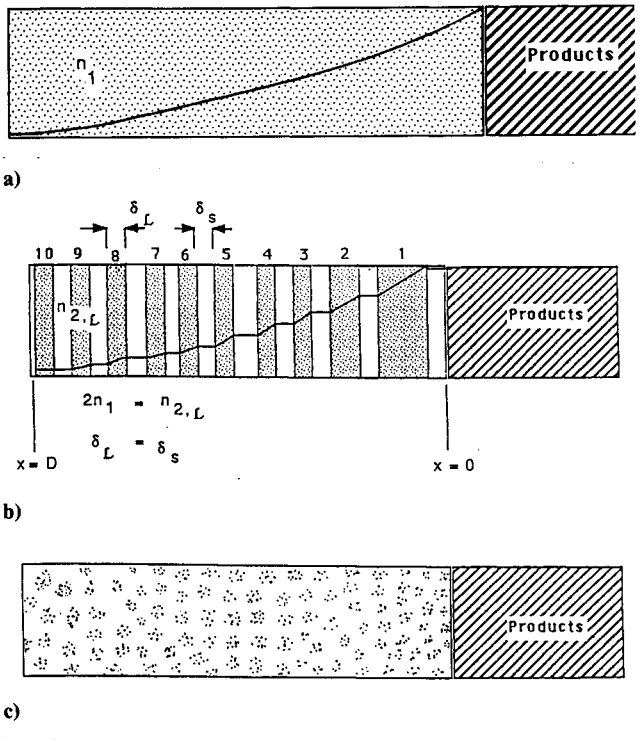

Fig. 3 Radiation attenuation patterns for several modes of particle-cloud flame propagation. Overall equivalence ratio ϕ_0 is the same for all cases: a) uniform particle cloud; b) acoustically segregated particle cloud; and c) nonuniformly mixed particle cloud. For these illustrative cases, combustion progresses from right to left.

Figure 3 shows the attenuation patterns for the radiative fields associated with several different modes of flame propagation. The first case of Fig. 3 corresponds to a uniform cloud of (lycopodium) particulates in air, subject to an initial radiative flux density I_0 (incident from the right) originating from hot, combustion products. For the same initial equivalence ratio ϕ_0, the second case of Fig. 3 corresponds to an acoustically segregated system of laminae,[6] where the equivalence ratio prior to acoustic segregation is also ϕ_0. Particle segregation derives from flame-induced acoustic excitation[6] of the Kundt's tube phenomenon.[7,8] The third case of Fig. 3 corresponds to a microscopically nonuniform mixture, which is macroscopically uniform at the same equivalence ratio ϕ_0.

The decay of the combustion product radiation, within the upstream (cold) regime, is macroscopically similar for all three cases if 1) the optical penetration distance of the radiative flux density is large compared to the scales of the characteristic spatial inhomogeneities of cases B and C; and 2) the system is adiabatic, corresponding to very large experimental apparatus and one-dimensional transport phenomena.

Quasisteady flame propagation has been observed for each of the three cases cited.[6] In order to characterize the radiative structure of the upstream (unburned) regime, it is necessary to know the optical attenuation characteristics of the unburned fuel particles. It is also necessary to know the vaporization-pyrolysis characteristics of the fuel particles if the radiative flux density is to be known in the flame regimes where these processes occur. Finally, it is necessary to know particle sizes and characteristics in the regimes where rapid oxidation of the gaseous vaporization-pyrolysis products leads to the final combustion products.

For unburned lycopodium particulates of 27-μm diameter, we have determined[7,9] that the particles appear to be black in the infrared and that the attenuation law is given by

$$I_t = I_0 \exp(-53.0\, CX) \tag{1}$$

where

I_t = transmitted radiative flux density, kW/m^2
I_0 = incident radiative flux density, kW/m^2
C = particle concentration, kg/m^3
X = space variable, m

Our experimental studies of the vaporization-pyrolysis kinetics of lycopodium reveal that these processes are largely complete at temperatures of about 650–700 K. It is also found that the autoignition temperatures for a cloud of lycopodium particulates lie in about the same range. Accordingly, the high-temperature oxidative regime of a flame (for each of the three cases cited) contains particulates <6-μm diameter (ash particulates).

Based on the above considerations, the radiative flux density for the case A lycopodium-air flame (uniform cloud case) can be represented as shown in Fig. 4. In the temperature range $T_0^* \le T \le T_1$ vaporization-pyrolysis rates are small and Eq. (1) applies, where $I_0 = I_{0,1}$, the value of I at $T = T_1$. In the vaporization-pyrolysis regime, $T_1 \le T \le T_2$, vaporization-pyrolysis rates are found to obey a kinetic law of the form

$$\frac{dm_p}{dt} = k(m_p - m_{p,0}) \exp\left(\frac{-E_v}{RT}\right) \tag{2}$$

The essential vaporization-pyrolysis range for lycopodium particulates lies in the range defined by $T_1 \approx 500$ K and $T_2 \approx 700$ K, where

m_p = particle mass, kg
$m_{p,0}$ = nonvolatile particle mass, kg
k = pre-exponential factor, s^{-1}
E_v/R = effective activation temperature for vaporization-pyrolysis, K

For quasisteady flame propagation at a burning velocity U, Eq. (2) can be employed to obtain an equation for the particle diameter in the vaporization-pyrolysis regime:

$$\frac{d}{dx} d_p = \frac{-1}{3U}\left(d_p - \frac{d_{p,0}^3}{d_p^2}\right) k \exp\left(\frac{-E_v}{RT}\right) \tag{3}$$

The appropriate attenuation law for the vaporization-pyrolysis regime can be written as follows:

$$I_t = I_{0,2} \exp\left(-\gamma_1 CX \frac{d_p^2}{d_{p,0}^2}\right) f\left(\frac{d_p}{d_{p,0}}\right) \tag{4}$$

Table 1 Initial lamina temperature calculated for the lycopodium-air system under conditions where $\phi_0 = 0.5$, $\phi_1 = 1.0$, and $\delta_1 = \delta_2$ (first-order calculation). Calculated value of τ_a is 25.3 ms.

Cell no., j	Temperature at $t = 0$, K	Cell no., j	Temperature at $t = 0$, K	Cell no., j	Temperature at $t = 0$, K
14	298	9	406	4	552
13	317	8	432	3	586
12	337	7	460	2	622
11	359	6	489	1	660
10	382	5	520	—	—

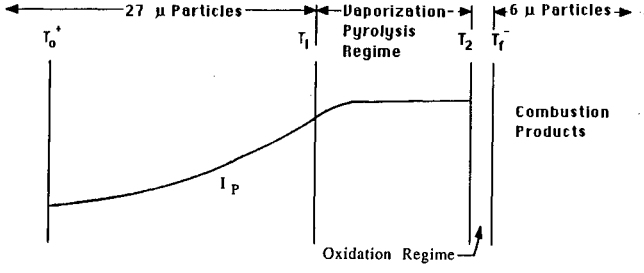

Fig. 4 Radiative flux structure for uniformly mixed lycopodium-air flame.

For virtually all of the vaporization-pyrolysis regime, $(d_p/d_{p,0})^2 \gg 1$ and $f = 1.0$. For cases where $(d_p/d_{p,0})^2 \approx 1$, f values are to be calculated by methods described elsewhere.[9]

Because the vaporization-pyrolysis is essentially complete at a temperature T_2, which is much lower than the flame temperature T_f, the very thin oxidation regime contains particulates that are nonvolatile (ash). For lycopodium, the nonvolatile ash has an optical extinction cross section that is only about 4% of that value associated with the original lycopodium particle. Because of the near-adiabatic nature of this system, the Mie scattering in the infrared is essentially forward scattering. Also, $(T_f/T_2) \sim 3$ and reradiation and scattering effects may be taken to be small for the one-dimensional (adiabatic) case.

In the thin, high-temperature oxidation regime, $T_2 \leq T \leq T_f$, radiative attenuation is small. Correspondingly, $I_{0,f} = I_0$, which is equal to the radiative flux density (originating from the combustion products) in the negative x direction.

The quasisteady flame equations for representation of the system require that the local volumetric radiative heating rate be specified everywhere on the regime $T_0 \leq T \leq T_f$. For the adiabatic case, the combustion products are considered to be arbitrarily opaque and at temperature T_f. Accordingly, the values I_0, C, and E_v are known and the local radiative energy deposition rate, dI/dx, is also known in terms of the above-cited parameters and equations. The physical ingredients needed to utilize the quasisteady flame equations, with radiation, are also known.

The second case illustrated in Fig. 3 corresponds to a novel form of flame propagation reported by us only recently.[6] In this form of flame propagation, lycopodium-air flames in long flame tubes have been observed (in reduced-gravity experiments aboard NASA Lewis Research Center Learjets during 20-s Keplerian trajectories) to acoustically excite the Kundt's tube phenomenon. These chattering flames[6] propagate as a series of radiatively induced autoignitions, with a characteristic autoignition time that is associated with the radiative heating of the partially absorbing particle cloud. The particle-laden laminae of the Kundt's tube phenomenon are radiatively brought to autoignition by a radiative field whose optical penetration depth (≥ 0.1 m) is much greater than the Kundt's tube nonuniformity scale (≤ 0.01 m). A first-order theory for chattering flames has been developed and yields good agreement between observed[6] and calculated chattering-flame burning velocities. Higher-order calculations[10] show that the employed first-order assumption (of negligible small conductive-diffusive interactions between particle-laden laminae) is appropriate for laminae separations of the order of 0.01 m or greater (as employed in Ref. 6).

As noted earlier, on a spatial scale that is much larger than δ_s (the laminae spacings), the macroscopic features of the radiative fields for all three cases are essentially similar. However, it is necessary[6] that the particle concentrations associated with each of the radiatively heated Kundt's laminae be known. Although the overall equivalence ratio ϕ_0 is known a priori, the Kundt's tube phenomenon[6,8] creates alternate layers of particle-enriched and particle-depleted regimes. It can be shown directly from the above-noted optical attenuation properties that the radiative flux density transmitted by each lamina layer is given by

$$I_{t,j} = I_{t,j-1}\{\exp[-(j-1)\gamma C\delta_1] - \exp(-j\gamma C\delta_1)\} \qquad (5)$$

where $j = 1$ corresponds[6] to the lamina regime within which chemical autoignition occurs and $j > 1$ corresponds to the sequence of lamina regimes that are being radiatively pumped by the hot combustion products. In the $j = 2$ regime, the attenuation constant γ may be modified to take account of the vaporization-pyrolysis diminution of the particle diameter. This $j = 2$ effect is small. Within $j = 1$, particulates are essentially ash (< 6 μm), and at $j = 1$ autoignition trajectories of the supercritical vaporization-pyrolysis products are consummated in a time τ_a. As noted previously,[6,10] the considered quasisteady chattering-flame propagation is characterized experimentally and theoretically by τ_a. The calculated τ_a values derived from both first-order and from second-order calculations are given elsewhere,[10] for an overall equivalence ratio $\phi_0 = 0.5$. Table 1 lists the initial ($t = 0$) temperature values calculated for a set of 14 segregated particle laminae that are driven radiatively to autoignition in the $j = 1$ lamina.

The nonuniform radiative fields associated with the third case of Fig. 3 can vary substantially, depending on details of the particle-cloud nonuniformities, and is not analyzed here. It is to be noted, however, that we have observed flames for experimental cases, which satisfy the macroscopic uniformity criterion given earlier (scale of nonuniformity is small compared to the optical penetration depth). In this third case (of Fig. 2), local clusters of (enriched) particle concentrations are seen to autoignite, in consequence of radiative heating by the advancing, non-simply-connected flame structure.

Discussion

The overall energy equation for a combustible system that moves along an explosive trajector can be written as follows:

$$\rho c_p \frac{\partial T}{\partial t} = \nabla \cdot (\lambda \nabla T + I_{\text{rad}}) + \sum_{i=1}^{N} h_{fi}^0 \dot{W}_i''' \qquad (6)$$

where

ρ = density, kg/m^3
c_p = heat capacity, kJ/kg/K

λ = thermal conductivity, kW/m/K
I_{rad} = radiative flux density, kW/m^2
$\dot{W}_i'''$ = the rate of production of the ith chemical species by chemical and/or vaporization-pyrolysis processes, kg/m^3/s
$h^0_{f,i}$ = enthalpy of formulation of species i, kJ/kg

Thermophysical and chemical kinetic properties of a combustible system must be known in order to apply Eq. (6) to a numerical deduction of $T(x,t)$. For a large (near-adiabatic) flame system, flame temperature is deducible from thermodynamic considerations alone. This permits specification of the radiative flux density vector imposed on the reaction zone (upstream) structure by the arbitrarily thick combustion products. Where particle clouds play a role in flame phenomena, the optical attenuation properties of individual particles as well as the spatial distribution of the particles in the cloud must be known. This is required even for the case where optical and particle reradiation effects are small.

The optical attenuation properties of lycopodium particles have been measured[9] and incorporated, along with the adiabatic flame properties of lycopodium-air systems, and along with observed low-gravity particle-cloud spatial structures. These deductions have been employed in the autoignition time calculations reported in Refs. 6 and 10 and Table 1.

The several particle-cloud spatial distributions of Fig. 3 all correspond to the same ϕ_0 value and the same adiabatic flame temperature. The important radiative attenuation features appropriate to the utilization of Eq. (6) differ strikingly. Correspondingly, the general characteristics of these radiatively dominated flame properties also differ strikingly.

The observed low-gravity combustion processes all correspond to nonadiabatic processes. Flame propagation in modest-sized flame tubes entails some radiative losses in the radial directions. Postcombustion cooling of combustion products corresponds to hot combustion products that are less emissive than those considered for the adiabatic case. Accordingly, first- and second-order adiabatic representation of chattering flames are but a first step in a more general (nonadiabatic) representation of the characteristics of these flames. A similar statement can be made about each of the other two observed low-gravity modes of flame propagation. The current theoretical program at the University of California, San Diego, emphasizes analysis of the nonadiabatic characteristics of these several modes of low-gravity, particle-cloud flame propagation.

Acknowledgment

These studies were performed under sponsorship of NASA.

References

[1]Berlad, A. L., "Combustion Studies in Microgravity," *Progress in Astronautics and Aeronautics: Opportunities for Academic Research in a Low-Gravity Environment,* Vol. 108, edited by G. A. Hazelrigg and J. M. Reynolds, AIAA, New York, 1986, p. 201.

[2]Ross, H., Facca, L., Tangirala, V., and Berlad, A. L., "Feasibility of Reduced-Gravity Experiments Involving Quiescent, Uniform Particle-Cloud Combustion," NASA TM-101371, March 1989.

[3]Berlad, A. L., "Combustion of Particle Clouds," *Progress in Astronautics and Aeronautics: Combustion Experiments in a Zero-Gravity Laboratory,* Vol. 73, edited by Thomas Cochran, AIAA, New York, 1981, p. 91.

[4]Berlad, A. L., and Joshi, N. D., "Gravitational Effects on the Extinction Conditions for Premixed Flames," *Acta Astronautica,* Vol. 12, 1985, p. 539.

[5]Berlad, A. L., "Combustion Studies in Low Gravity," *Progress in Astronautics and Aeronautics: Opportunities for Academic Research in a Low-Gravity Environment,* Vol. 108, edited by G. A. Hazelrigg and J. M. Reynolds, AIAA, New York, 1986, p. 205.

[6]Berlad, A. L., Ross, H., Facca, L., and Tangirala, V., "Particle-Cloud Flames in Acoustic Fields," *Combustion and Flame* (to be published).

[7]Berlad, A. L., "Particle-Cloud Combustion in Low Gravity," *Progress in Astronautics and Aeronautics: Materials and Fluid Sciences in Low Gravity*, Vol. 130, edited by J. N. Koster and R. L. Sani, AIAA, Washington, DC, 1990, p. 703.

[8]Lord Rayleigh, *The Theory of Sound*, Vol. II, Dover, New York, 1945, p. 57.

[9]Berlad, A. L., and Tangirala, V., "Reduced-Gravity Combustion of Particle Clouds," NASA CR-182299, Dec. 1988.

[10]Berlad, A. L., Tangirala, V., Ross, H., and Facca, L., "Particle-Segregation Effects on the Combustion Safety of Dust-Containing Systems," *Proceedings of the 12th International Colloquium on the Dynamics of Explosions and Reactive Systems,* July 1989; see also *Progress in Astronautics and Aeronautics: Dynamics of Reactive Systems and Explosions,* edited by A. L. Kuhl, J. C. Leyer, and A. Borisov, AIAA, Washington, DC (to be published).